

Selective Pressures to Maintain Attachment Site Specificity of Integrative and Conjugative Elements

Kayla L. Menard, Alan D. Grossman*

Department of Biology, Massachusetts Institute of Technology, Cambridge, Massachusetts, United States of America

Abstract

Integrative and conjugative elements (ICEs) are widespread mobile genetic elements that are usually found integrated in bacterial chromosomes. They are important agents of evolution and contribute to the acquisition of new traits, including antibiotic resistances. ICEs can excise from the chromosome and transfer to recipients by conjugation. Many ICEs are site-specific in that they integrate preferentially into a primary attachment site in the bacterial genome. Site-specific ICEs can also integrate into secondary locations, particularly if the primary site is absent. However, little is known about the consequences of integration of ICEs into alternative attachment sites or what drives the apparent maintenance and prevalence of the many ICEs that use a single attachment site. Using *ICEBs1*, a site-specific ICE from *Bacillus subtilis* that integrates into a tRNA gene, we found that integration into secondary sites was detrimental to both *ICEBs1* and the host cell. Excision of *ICEBs1* from secondary sites was impaired either partially or completely, limiting the spread of *ICEBs1*. Furthermore, induction of *ICEBs1* gene expression caused a substantial drop in proliferation and cell viability within three hours. This drop was dependent on rolling circle replication of *ICEBs1* that was unable to excise from the chromosome. Together, these detrimental effects provide selective pressure against the survival and dissemination of ICEs that have integrated into alternative sites and may explain the maintenance of site-specific integration for many ICEs.

Citation: Menard KL, Grossman AD (2013) Selective Pressures to Maintain Attachment Site Specificity of Integrative and Conjugative Elements. *PLoS Genet* 9(7): e1003623. doi:10.1371/journal.pgen.1003623

Editor: Diarmaid Hughes, Uppsala University, Sweden

Received: December 12, 2012; **Accepted:** May 27, 2013; **Published:** July 18, 2013

Copyright: © 2013 Menard, Grossman. This is an open-access article distributed under the terms of the Creative Commons Attribution License, which permits unrestricted use, distribution, and reproduction in any medium, provided the original author and source are credited.

Funding: This work was supported, in part, by Public Health Service grant GM050895 to ADG. The funders had no role in study design, data collection and analysis, decision to publish, or preparation of the manuscript.

Competing Interests: The authors have declared that no competing interests exist.

* E-mail: adg@mit.edu

Introduction

Integrative and conjugative elements (ICEs, also known as conjugative transposons) are mobile genetic elements that encode conjugation machinery that mediates their transfer from cell to cell. Most characterized ICEs were identified because they carry additional genes that confer phenotypes to the host cell. These can be genes involved in pathogenesis, symbiosis, and antibiotic resistances, among others [1]. ICEs are typically found integrated in the host bacterial chromosome and can excise to form a circular product that is the substrate for conjugation. Their ability to spread to other organisms through conjugation makes ICEs important agents of horizontal gene transfer in bacteria, and they appear to be more prevalent than plasmids [2]. ICEs can also facilitate transfer (mobilization) of other genetic elements [1,3,4].

Some ICEs have a specific integration (attachment or insertion) site in the host genome whereas others are more promiscuous and can integrate into many locations. For example, SXT, an ICE in *Vibrio cholera* has one primary site of integration in the 5' end of *prfC* [5]. In contrast, Tn916 has a preference for AT-rich DNA in many different hosts and integrates into many different chromosomal sites [6,7]. Each strategy for integration has its benefits. The more promiscuous elements can acquire a wider range of genes adjacent to the integration sites, and their spread is not limited to organisms with a specific attachment site. On the other hand, site-specific elements are much less likely to disrupt important genes.

The attachment site for these elements is typically in a conserved gene, often a tRNA gene [8,9]. If sequences at the end of the integrating element are identical with the 3' end of the gene (which is often the case), then gene function is not disrupted. Integration into conserved genes makes it likely that many organisms will have a safe place for these elements to integrate. We wished to learn more about the ability of site-specific ICEs to integrate into secondary integration (or attachment) sites, particularly if the primary site is not present in a genome. We wondered if an ICE could function normally in a secondary site and if there was any effect on the host.

We used *ICEBs1* of *Bacillus subtilis* to analyze effects of integration into secondary attachment sites. *ICEBs1* is a site-specific conjugative transposon that is normally found integrated into a tRNA gene (*trnS-leu2*) [10,11]. *ICEBs1* is approximately 20 kb (Figure 1), and many of its genes are similar to genes in other ICEs, including those in Tn916 [11,12], the first conjugative transposon identified [13,14]. It is not known what properties or advantages *ICEBs1* confers on host cells, and naturally occurring *ICEBs1* is not known to carry genes involved in antibiotic resistances, virulence, or metabolism. However, because of the conservation of many of its functions, the ease of manipulating *B. subtilis*, and the high efficiency of experimental induction of gene expression, *ICEBs1* is extremely useful for studying basic and conserved properties of ICEs.

Induction of *ICEBs1* gene expression leads to excision from the chromosome in >90% of the cells, autonomous rolling-circle

Author Summary

Integrative and conjugative elements (ICEs) are mobile genetic elements that transfer DNA between bacteria, driving bacterial evolution and the acquisition of new traits, including antibiotic resistances. ICEs normally reside integrated in a host genome, but can excise and transfer to recipient cells. Many ICEs are site-specific, predominantly integrating into a single “attachment” site. Others are more promiscuous, capable of integrating into many different sites. Little is known about the consequences of a site-specific ICE integrating into an alternative attachment site, or the selective pressures that maintain the specificity of integration for ICEs with a single attachment site. We found that integration of *ICEBs1*, a site-specific ICE in *Bacillus subtilis*, into alternative attachment sites was detrimental to both *ICEBs1* and the host cell. Excision of *ICEBs1* from alternative attachment sites was reduced or eliminated, thereby limiting mobility of the element. In addition, when *ICEBs1* gene expression was activated, cell proliferation and viability dropped if *ICEBs1* was in an alternative attachment site. This drop was due to autonomous replication of *ICEBs1* that was stuck in the host chromosome. These detrimental effects likely provide strong selective pressure to maintain attachment site specificity of *ICEBs1* and likely many other site-specific ICEs.

replication of *ICEBs1*, and mating in the presence of appropriate recipients [10,11,15]. After excision from the chromosome, autonomous replication of *ICEBs1* is needed for its stability during cell growth and division [15]. In addition, excision is not needed for replication; *ICEBs1* that is unable to excise from the chromosome undergoes autonomous unidirectional replication following induction of *ICEBs1* gene expression [15]. At least some other ICEs appear to undergo autonomous replication [1,16–18]. In addition, the genes in *ICEBs1* that are required for autonomous replication are conserved [19]. Based on these observations and the properties of *ICEBs1*, we suspect that many ICEs undergo rolling circle replication and use the origin of transfer as an origin

of replication and the cognate conjugative relaxase as a replicative relaxase [3,19].

Our aim was to examine the physiological consequences of integration of *ICEBs1* into secondary attachment sites. Previous work showed that in the absence of its primary attachment site (*attB* in the gene for tRNA-leu2), *ICEBs1* integrates into secondary attachment sites [10]. Seven different sites were identified and characterized previously, providing insight into the chromosomal sequences needed for integration [10]. Work presented here extends these findings by identifying additional secondary sites, evaluating the ability of *ICEBs1* to excise from these sites, and determining the effects of integration at these sites on host cells. Our results indicate that integration of *ICEBs1* into secondary integration sites is deleterious to *ICEBs1* and to the host cell. Excision and spread of *ICEBs1* from the secondary sites was reduced or eliminated and there was a drop in cell viability due to autonomous replication of *ICEBs1* that was defective in excision. These effects likely provide strong selective pressure for insertions into sites from which *ICEBs1* can excise and against the propagation of insertions in secondary sites.

Results

Identification of secondary sites of integration of *ICEBs1*

We identified 27 independent insertions of *ICEBs1* into secondary integration sites in the *B. subtilis* chromosome. Briefly, these insertions were identified by: 1) mating *ICEBs1* into a recipient strain deleted for the primary attachment site *attB* (located in the tRNA gene *tmS-leu2*), 2) isolating independent transconjugants, and 3) determining the site of insertion in each of 27 independent isolates. The frequency of stable acquisition of *ICEBs1* by strains missing *attB* was reduced to ~0.5–5% of that of strains containing *attB* {Materials and Methods, and [Materials and Methods, and 10]}.

There were 15 different secondary integration sites for *ICEBs1* among the 27 independent transconjugants (Figure 2). Seven of the 15 sites were described previously [10], and eight additional sites are reported here. There appears to be no absolute bias for

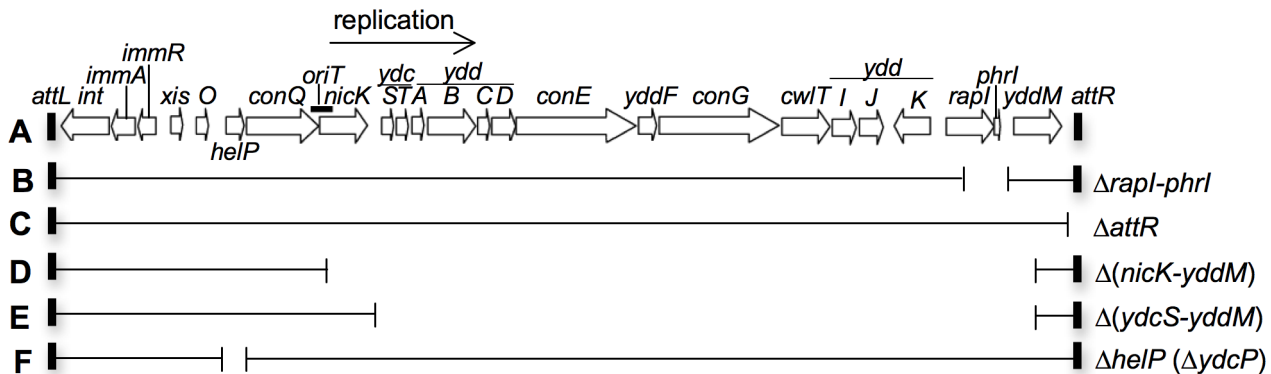


Figure 1. Map of *ICEBs1* and its derivatives. **A.** The linear genetic map of *ICEBs1* integrated in the chromosome. Open arrows indicate open reading frames and the direction of transcription. Gene names are indicated above or below the arrows. The origin of transfer (*oriT*) is indicated by a thick black line overlapping the 3' end of *conQ* and the 5' end of *nick*. *oriT* functions as both the *ICEBs1* origin of transfer and origin of replication [15,23]. The thin black arrow indicates the direction of *ICEBs1* rolling-circle replication. The small rectangles at the ends of *ICEBs1* represent the 60 bp direct repeats that contain the site-specific recombination sites in the left and right attachment sites, *attL* and *attR*, that are required for excision of the element from the chromosome. **B–F.** Various deletions of *ICEBs1* were used in this study. Thin horizontal lines represent regions of *ICEBs1* that are present and gaps represent regions that are deleted. Antibiotic resistance cassettes that are inserted are not shown for simplicity. **B.** *rapI* and *phrI* are deleted and a kanamycin resistance cassette inserted. **C.** The right attachment site (*attR*) is deleted and a tetracycline resistance cassette inserted. **D.** The genes from the 5' end of *nick* and into *yddM* are deleted and a chloramphenicol resistance cassette inserted. **E.** The genes from the 5' end of *ydcS* and into *yddM* are deleted and a chloramphenicol resistance cassette inserted. **F.** The entire coding sequence of *helP* (previously known as *ydcP*) and 35 bp in the *helP-ydcQ* intergenic region is removed. There is no antibiotic resistance cassette in this construct. doi:10.1371/journal.pgen.1003623.g001

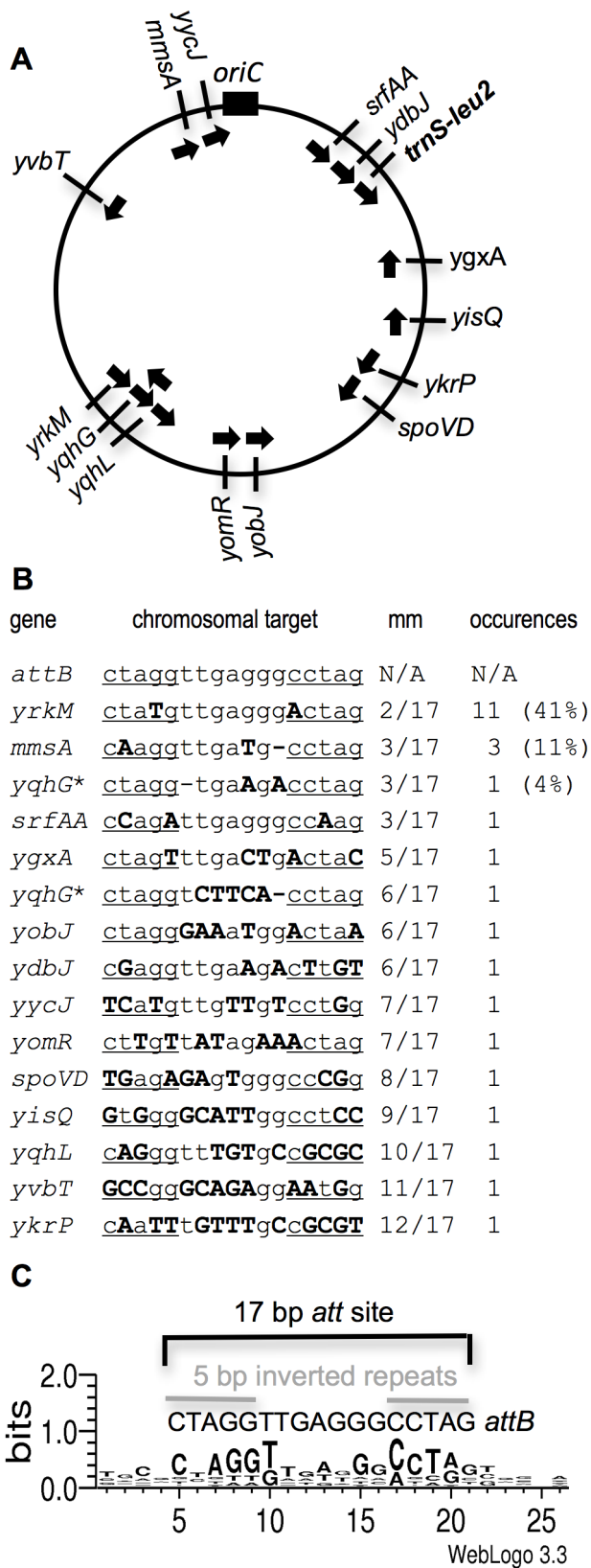


Figure 2. Map and DNA sequence of the primary and 15 secondary integration sites for ICEBs1. **A.** Approximate position of the primary and 15 secondary ICEBs1 integration sites on the *B. subtilis* chromosome. The circle represents the *B. subtilis* chromosome with the origin of replication (*oriC*) indicated by the black rectangle at the top.

The slash marks represent the approximate location of the ICEBs1 insertion site. The name of the gene near which (*ygxA*) or into which (all other locations) ICEBs1 inserted is indicated on the outside of the circle. The arrows on the inside of the circle indicate the direction of ICEBs1 replication for each insertion. *trnS-leu2* (in bold) contains the primary ICEBs1 integration site *attB*. **B.** DNA sequence of the primary and 15 secondary integration sites. The gene name is indicated on the left, followed by the DNA sequence (chromosomal target). The primary attachment site (*attB*) is a 17 bp sequence with 5 bp inverted repeats (underlined) separated by a 7 bp spacer. Mismatches from *attB* are indicated in bold, capital letters. "mm" indicates the number of mismatches from the primary 17 bp *attB*. "occurrences" indicates the number of independent times an insertion in each site was identified. Percentages of the total (27) are indicated in parenthesis. The * next to *yqhG* indicates that two different ICEBs1 insertions were isolated in this gene, once in each orientation. **C.** Sequence logo of the ICEBs1 secondary attachment sites. Using WebLogo 3.3 [21], we generated a consensus motif of the 26 bases surrounding the insertion site of the 15 secondary insertion sites for ICEBs1. For comparison, the primary attachment site for ICEBs1 is a 17 bp region with 5 bp inverted repeats and a 7 bp spacer region in the middle [10]. The size of each nucleotide corresponds to the frequency with which that nucleotide was observed in that position in the secondary attachment sites. doi:10.1371/journal.pgen.1003623.g002

the orientation of ICEBs1 insertions with respect to the direction of the replication forks, although 10 of the 15 insertions were oriented such that the direction of ICEBs1 replication was co-directional with the direction of the chromosomal replication forks (Figure 2A). Of the 27 independent transconjugants, 11 (41%) had ICEBs1 inserted in a site in *yrkM* (designated *yrkM::ICEBs1*) (Figure 2B), a gene of unknown function. Three of the 27 (11%) transconjugants had ICEBs1 inserted in a site in *mmsA* (encoding an enzyme involved in myo-inositol catabolism [20]). The site in *yrkM* is the most similar to the primary attachment site *attB*, differing by two base pairs. The site in *mmsA* differs from *attB* by three base pairs (Figure 2B). Two insertions were in a site in *yqhG*, although in opposite orientations. These are counted as two different sites since the sequence in each orientation is different (Figure 2B). The remaining 11 insertions were in unique sites, either in genes or intergenic regions (Figure 2B). None of the identified insertions caused a noticeable defect in cell growth in rich (LB) or defined minimal medium when ICEBs1 was repressed. Furthermore, none of the insertions were in tRNA genes (including redundant, nonessential tRNA genes) that are common integration sites for many ICEs [8,9].

Some of the secondary insertion sites were similar to and others quite different from the primary ICEBs1 attachment site (*attBICEBs1*, or simply *attB*). *attB* contains a 17 bp stem-loop sequence consisting of a 5 bp inverted repeat separated by 7 bp (Figure 2C). We aligned and compared the sequences of the 15 different secondary attachment sites and searched for a common motif using WebLogo 3.3 (<http://weblogo.threeplusone.com/>) [21]. For each secondary attachment site, we provided an input of 26 bp that included the region of the stem-loop sequence (17 bp, inferred from the sequence of *attB*) and a few base pairs upstream and downstream. The conserved sequences were largely in the 17 bp that were originally proposed to comprise *attB* [10], including several positions in the loop region of the stem-loop sequence, the 5 bp inverted repeats, and perhaps 1–2 additional base pairs downstream of the stem-loop (Figure 2C). There was considerable sequence diversity among the 15 secondary integration sites and the primary site *attB*, and no single position was conserved in all the secondary sites (Figure 2B). In some cases (e.g., insertions in *yrkM*, *mmsA*, *yqhG*, and *srfAA*) there are only 2–3 base pairs that are different between the secondary site and *attB*. In contrast, insertion sites in *yqhL*, *yvbT*, and *ykrP* have 10–12

mismatches (out of 17 bp) from the sequence of *attB* (Figure 2B). These results indicate that in the absence of the primary integration site in *trmS-leu2*, *ICEBs1* can integrate into many different sites throughout the genome, albeit at a lower efficiency [10]. Based on the diversity of the observed secondary attachment sites and the number of sites identified only once, it is clear that we have not identified all of the possible secondary integration sites for *ICEBs1*.

Integration into the secondary site in *ykrM* in the presence of a functional *attB*

We wondered if *ICEBs1* could insert into a secondary site in cells in which the primary site, *attB*, is intact. To test this, *ICEBs1* (from donor strain KM250) was transferred by conjugation to an *ICEBs1*-cured recipient that contained *attB* (strain KM524). Transconjugants were selected on solid medium and $\sim 10^8$ independent transconjugants were pooled. DNA from the pooled transconjugants was then used as a template for quantitative real-time PCR (qPCR) with primers that detected *ICEBs1* integrated into *ykrM* (the most frequently used secondary site). We found that the frequency of integration into *ykrM* was $\sim 10^{-4}$ to 10^{-3} of that into *attB*. As a control, we performed reconstruction experiments. Known amounts of DNA from two strains, one containing an insertion in *ykrM* (strain KM72), and the other containing an insertion in *attB* (strain AG174) were mixed and used as a template in qPCR, analogous to the experiment with DNA from the pooled transconjugants. These reconstruction experiments validated the results determined for the frequency of insertion into *ykrM*.

Excision of *ICEBs1* from secondary integration sites is reduced

We wished to determine if there were any deleterious consequences of integration of *ICEBs1* into secondary attachment sites. We found that although *ICEBs1* integrated into the secondary integration sites, excision from all of the secondary sites we analyzed was reduced or eliminated. We monitored excision from seven of the secondary sites by overexpressing the activator of *ICEBs1* gene expression, RapI, from a regulated promoter (P_{xyl-*rapI*}) integrated in single copy in the chromosome at the nonessential gene *amyE* (Materials and Methods). Overproduction of RapI induces *ICEBs1* gene expression [11,22] and typically results in excision of *ICEBs1* from *attB* in >90% of cells within 1–2 hrs [10,15]. Following a similar protocol as described for monitoring excision from *attB* [11,15,22], we performed qPCR using genomic DNA as template and primers designed to detect the empty secondary attachment site that would form if the element excised. In a positive control, excision of *ICEBs1* from *attB* occurred in >90% of cells within two hours after expression of the activator RapI (Figure 3A, wt). In a negative control, excision of an *ICEBs1* $\Delta attR$ mutant (Figure 1C), integrated in *attB*, was undetectable (Figure 3A, $\Delta attR$). Excision from four of the sites tested, *ykrM*, *mmsA*, *sfAA*, and *yycJ*, was reduced yet still detectable, ranging from 4% to 15% of that of *ICEBs1* from *attB*. Excision from the other three sites tested, *yvbT*, *spoVD*, and *ykrP*, was undetectable (Figure 3A), similar to what we observed for *ICEBs1* $\Delta attR$, the excision-defective control. In general, the secondary integration sites that are most divergent from *attB* had the least amount of excision (Table 1).

These findings indicate that integration of *ICEBs1* into sites other than *attB* causes a reduction, sometimes quite severe, in the ability of the element to excise. Because excision is required for transfer of a functional ICE, this reduced excision will limit the spread of *ICEBs1* that has inserted into secondary sites from which it cannot escape.

Decreased conjugation of *ICEBs1* from secondary sites

We measured the mating efficiencies of *ICEBs1* following excision from the four secondary attachment sites from which excision was reduced but detectable. Excision of *ICEBs1* is required for transfer of the element to recipient cells. Thus, if the *ICEBs1* circle is stable, then the mating efficiencies should be proportional to the excision frequency. The mating efficiencies of *ICEBs1* from *ykrM* and *sfAA* were ~ 2 –5% of that of *ICEBs1* from *attB*. Likewise, the excision frequencies of *ICEBs1* inserted in *ykrM* and *sfAA* were $\sim 5\%$ of those of *ICEBs1* in *attB*. These results indicate that for *ICEBs1* integrated in *ykrM* and *sfAA*, the mating efficiencies were approximately what was expected from the reduced excision frequencies.

In contrast, the mating efficiencies of *ICEBs1* that excised from *mmsA* or *yycJ* were reduced beyond what would be expected from the already lowered excision frequency. In both cases, the excision frequencies were $\sim 15\%$ of that of *ICEBs1* integrated in *attB*. However, the mating efficiencies were $\sim 0.2\%$ of that of *ICEBs1* from *attB*, a 75-fold difference. Based on this result, we postulated that the reduced mating efficiency relative to the excision frequency was indicative of a reduction in the amount of circular *ICEBs1*.

Reduced levels of circular *ICEBs1* from secondary sites that generate a heteroduplex

We measured the relative amounts of circular *ICEBs1* after excision from *ykrM*, *sfAA*, *mmsA*, and *yycJ*, the four insertions with reduced but detectable excision, using qPCR primers designed to detect only the circular form of *ICEBs1*. The relative amounts of each circle were compared to the relative amount of the empty secondary attachment site from which *ICEBs1* excised. Measurements were made two hours after induction of *ICEBs1* gene expression (overproduction of RapI).

As expected, the ratio of the amounts of the circular form to the empty attachment site was about the same for insertions in *ykrM* and *sfAA* as for an insertion in *attB* (Figure 3B). In contrast, the ratio of the circle to the empty attachment site for *mmsA* and *yycJ* was significantly less than that for wild type (Figure 3B). Comparing the total amount of the *ICEBs1* circle from *mmsA* and *yycJ* to that from *attB* indicated that there was approximately 0.3% as much circle from each site as from *attB*. This decrease in the amount of *ICEBs1* circle is consistent with and likely the cause of the drop in mating efficiency to approximately 0.2% of that of *ICEBs1* from *attB*.

The decrease in the amount of circular *ICEBs1* from *mmsA* and *yycJ* is likely due to the generation of a heteroduplex in the attachment site on the circular *ICEBs1*. The *ICEBs1* attachment site contains a 17 bp sequence with a 7 bp spacer region between 5 bp inverted repeats. Integrase-mediated site-specific recombination occurs in the 7 bp spacer (the crossover region) [10] (Figure 3C). If the 7 bp region in a chromosomal attachment site is different from that in *ICEBs1*, as is the case for *mmsA* and *yycJ*, then integration and host replication will create left (*attL*) and right (*attR*) ends that have different crossover regions (Figure 3D). Upon excision, these elements are predicted to contain a heteroduplex in the attachment site on the excised circular *ICEBs1*. Of the four insertions that have readily detectable excision frequencies, two (*mmsA* and *yycJ*) are predicted to form a heteroduplex and two (*ykrM* and *sfAA*) are not. In the case of *mmsA::ICEBs1*, the left and right ends are known to have different sequences [10].

Together, our results indicate that excision of *ICEBs1* from secondary sites from which a heteroduplex is formed leads to lower levels of the circular *ICEBs1* heteroduplex and a reduction in the ability of *ICEBs1* to transfer to other cells. We do not yet know

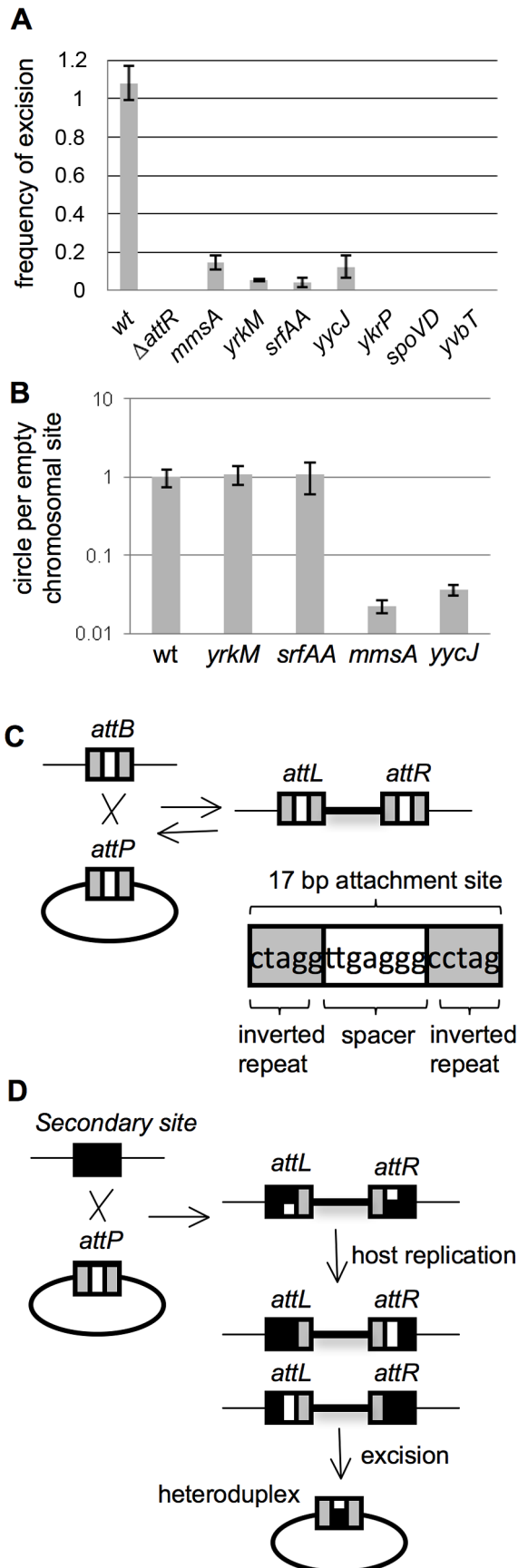


Figure 3. Excision of ICEBs1 from secondary attachment sites.

A–B. Excision frequencies and relative amounts of the excision products (circular ICEBs1 and empty chromosomal site) were determined as described in Materials and Methods. Cells were grown in defined minimal medium with arabinose as carbon source. Products from excision were determined two hours after addition of xylose to induce expression of P_{xyl}-*rapI* to cause induction of ICEBs1 gene expression. Primers for qPCR were unique to each attachment site. Strains used include: wt, that is, ICEBs1 inserted in *attB* (CAL874); $\Delta attR$, ICEBs1 integrated in *attB*, but with the right attachment site deleted and ICEBs1 unable to excise (Figure 1) (CAL872); *mmsA*::ICEBs1 (KM70); *yrkM*::ICEBs1 (KM72); *srfAA*::ICEBs1 (KM141); *ycyJ*::ICEBs1 (KM132); *ykrP*::ICEBs1 (KM77); *spoVD*::ICEBs1 (KM130); *yvbT*::ICEBs1 (KM94). Each strain was assayed at least three times (biological replicates) and qPCR was done in triplicate on each sample. Error bars represent standard deviation. **A.** Frequency of excision of ICEBs1 from the indicated site of integration. The relative amount of the empty chromosomal attachment site was determined and normalized to the chromosomal gene *cotF*. Data were also normalized to a strain with no ICEBs1 (JMA222), which represents 100% excision. **B.** Relative amount of circular ICEBs1 compared to the amount of empty chromosomal attachment site for the indicated insertions. The relative amount of the ICEBs1 circle, normalized to *cotF*, was divided by the relative amount of the empty attachment site, also normalized to *cotF*. These ratios were then normalized to those for wild type. **C.** Cartoon of integration of ICEBs1 into its primary bacterial attachment site *attB*. *attB* is identical to the attachment site on ICEBs1, *attICEBs1*. They consist of a 17 bp region with 5 bp inverted repeats (gray boxes) on each side of a 7 bp spacer region (white box). During integration and excision, a recombination event occurs in the 7 bp spacer (crossover) region [38]. **D.** Cartoon of integration of ICEBs1 into secondary integration sites. A secondary integration site is indicated with a black box. When ICEBs1 integrates into a secondary site, the crossover regions in *attICEBs1* and that of the secondary site are not necessarily identical, potentially creating a mismatch. This mismatch, if not repaired, will be resolved by host replication, generating left and right ends with different crossover sequences. Excision would then create a circular ICEBs1 with a heteroduplex in the attachment site on ICEBs1.

doi:10.1371/journal.pgen.1003623.g003

Table 1. Summary of properties of several ICEBs1 insertions in secondary attachment sites.

Insertion site (#mm) ^a	Excision frequency ^b	Viability ^c	<i>dinC-lacZ</i> ^d
<i>attB</i>	1.0	1.0	1.0
<i>yrkM</i> (2)	0.06	0.030	34
<i>mmsA</i> (3)	0.15	0.14	6.1
<i>srfAA</i> (3)	0.04	0.10	8.7
<i>ycyJ</i> (7)	0.12	0.073	N.D.
<i>spoVD</i> (8)	<10 ⁻⁴	0.010	N.D.
<i>ykrP</i> (12)	<10 ⁻⁴	0.040	4.1
<i>yvbT</i> (11)	<10 ⁻⁴	0.0038	24
$\Delta attR$	<10 ⁻⁴	0.092	6.7

^asite of insertion of ICEBs1; #mm indicates the number of mismatches between the insertion site and *attB* (illustrated in Figure 2).

^bexcision frequency measured as the empty attachment site 2 hrs after induction of ICEBs1 gene expression; normalized to wt; same data as in Figure 3, except that here data is normalized to wt (*attB*). Excision frequency from *attB* was 1.

^ccell viability normalized to ICEBs1 at *attB*; same data as in Figure 4. Viability of ICEBs1 at *attB* was 0.9 of uninduced.

^dexpression of damage inducible gene *dinC-lacZ*, normalized to that of cells with ICEBs1 at *attB*; data from Figure 6. β -galactosidase specific activity of ICEBs1 at *attB* was 0.3.

doi:10.1371/journal.pgen.1003623.t001

what causes the lower amounts of the *ICEBs1* heteroduplex. Loss of the DNA mismatch repair gene *mutS* did not alter the instability of the *ICEBs1* heteroduplex (unpublished results), indicating that mismatch repair is not solely responsible for this effect. Nonetheless, the overall reduction in transfer is due to both decreased excision and further decreased amounts of the excised element. Both of these defects provide barriers to the spread of *ICEBs1* from secondary attachment sites.

ICEBs1 returns to *attB* following excision and conjugation from secondary sites

We found that when *ICEBs1* excises from a secondary site and transfers to wild type cells via conjugation it tends to integrate in the primary attachment site, *attB*, and not in a secondary site. Donors with *ICEBs1* in *yrkM*, *mmsA*, *ycj7*, and *sfAA* were crossed with a recipient (strain KM110) containing *attB* (and all known secondary sites). Individual transconjugants from each cross were isolated and tested by PCR for the presence of *ICEBs1* in *attB*. *ICEBs1* was present in *attB* in 9 of 10 transconjugants from *yrkM::ICEBs1* donors, 9 of 9 transconjugants from *mmsA::ICEBs1* donors, 9 of 10 transconjugants from *ycj7::ICEBs1* donors, and 10 of 10 transconjugants from *sfAA::ICEBs1* donors. In the two cases where *ICEBs1* was not in *attB*, it was not present in the secondary site from which it came. We confirmed, using PCR primers internal to *ICEBs1*, that *ICEBs1* was present in the transconjugants. Thus, we conclude that even if *ICEBs1* is able to excise from a secondary attachment site, there is a strong bias in returning to the primary site if that site is present in a transconjugant.

We also found that if *attB* is not present in recipients during conjugation, then *ICEBs1* integrates into a secondary attachment site, but with no apparent bias for the site from which it originated. We crossed donors with *ICEBs1* in *yrkM*, *mmsA*, and *sfAA* with a recipient missing *attB* (strain KM111), and tested individual transconjugants for integration into the cognate site from which *ICEBs1* excised in the donor. With the *yrkM::ICEBs1* donor, 1 of 6 transconjugants had *ICEBs1* in *yrkM*. With the *mmsA::ICEBs1* donor, none of the 10 transconjugants tested had *ICEBs1* integrated in *mmsA*. With the *sfAA::ICEBs1* donor, none of the four transconjugants tested had *ICEBs1* in *sfAA*. Together, these results indicate that *ICEBs1* has a strong preference to integrate into *attB*, even when it starts from a secondary site, and that if *attB* is not available, *ICEBs1* tends to go to a secondary site, with no apparent preference for the original location.

Decreased proliferation and viability of strains in which *ICEBs1* has decreased excision

We found that strains with *ICEBs1* in secondary integration sites had a decreased ability to form colonies when *ICEBs1* gene expression was induced. We measured colony forming units (CFUs) of several strains with excision-defective (meaning reduced or no detectable excision) *ICEBs1* insertions, including *ICEBs1* in secondary sites and *ICEBs1* $\Delta attR$ (in *attB*), both with and without induction of *ICEBs1* gene expression. We also measured CFUs of wild type *ICEBs1* (with normal excision frequencies) integrated at *attB* under similar conditions (Figure 4A). In the absence of RapI expression, when most *ICEBs1* genes are repressed, growth and viability of excision-defective strains were indistinguishable from that of excision-competent strains. In contrast, by three hours after induction of *ICEBs1* gene expression in excision-defective *ICEBs1* strains ($\Delta attR$ with *ICEBs1* in *attB*, or insertions in *mmsA*, *yrkM*, *sfAA*, *ycj7*, *spoVD*, *yvbT*, and *yrkP*), the number of CFUs was reduced compared to that of the excision-competent *ICEBs1* (in

attB) (Figure 4A). These results are consistent with previous observations that excision-defective *int* and *xis* null mutants have a viability defect when RapI is overproduced [10].

Induction of *ICEBs1* in several of the secondary integration sites (insertions in *mmsA*, *sfAA*, *ycj7* and *ICEBs1* $\Delta attR$ in *attB*) caused a drop in CFU/ml to $\sim 10\%$ of that of strains without *ICEBs1* induction or the strain with wild type *ICEBs1* at *attB* (Figure 4A). Induction of *ICEBs1* in other insertion sites (*yrkP*, *yrkM*, *spoVD*, *yvbT*) caused a more severe drop in viability. The differences in CFU/ml between induced and uninduced cells (three hours after induction) appeared to be the combined effects of both a defect in proliferation (cell division) and cell death (viability). At times ≥ 3 hrs after induction of *ICEBs1* gene expression, the number of CFU/ml dropped to below that before induction of gene expression, indicating that preexisting cells lost viability. For simplicity, we use “viability” to refer to both cell death and the decreased proliferation.

The drop in viability after induction of *ICEBs1* in the various insertions did not correlate with dissimilarity of the attachment sites to *attB* or to the amount of residual excision in the excision-defective strains. For example, the *ICEBs1* $\Delta attR$ mutant is completely unable to excise, and viability is $\sim 10\%$ three hours after induction of *ICEBs1* gene expression. In contrast, *ICEBs1* inserted into *yrkM* has about 5% excision after induction of *ICEBs1* gene expression and viability is $\sim 3\%$ (Table 1). Together, these results indicate that something about the specific locations of the insertions is likely causing the more extreme viability defect observed in some of the excision-defective *ICEBs1* strains.

One of the most extreme effects on viability after induction of *ICEBs1* gene expression is from the insertion in *yvbT*. Within three hours after induction of *ICEBs1* gene expression in the *yvbT::ICEBs1* strain, viability was $\sim 0.3\%$ of that of strains without *ICEBs1* induction or of the strain with excision-competent *ICEBs1* (Figure 4A). *yvbT* gene product is predicted to be similar to alkanal monooxygenases (luciferases). Insertion of *ICEBs1* in *yvbT* likely knocks out *yvbT* function, so it seemed possible that the loss of *yvbT* combined with induction of *ICEBs1* gene expression was causing the severe drop in viability. To test this hypothesis, we deleted *yvbT* in cells containing *ICEBs1* inserted into *mmsA* and tested for viability after induction of *ICEBs1* gene expression. There was no additional drop in viability of the *mmsA::ICEBs1* *yvbT* null mutant compared to the *mmsA::ICEBs1* secondary site alone (wild type *yvbT*), either with or without induction of *ICEBs1* gene expression. Based on these results, we conclude that the severe defect in viability of the *yvbT::ICEBs1* secondary site mutant was not due to the loss of *yvbT* function combined with induction of *ICEBs1* gene expression. It is also possible the severe drop in viability was due to production of a fragment of the *yvbT* gene product. This possibility seems highly unlikely because the putative fragment alone does not cause a phenotype, rather the drop in viability requires both induction and replication (see below) of *ICEBs1*. In addition, other insertions also caused a severe drop in viability and it is highly unlikely that each one of these is producing a toxic protein fragment.

We do not know what causes the more severe drop in viability in some insertions. However, the decrease in cell proliferation and viability caused by expression of *ICEBs1* in secondary attachment sites should provide selective pressure against the long term survival of these strains. The more severe the loss in viability, the stronger the selective pressure against long term survival of strains with insertions in these sites. Suppressor mutations that alleviate the drop in viability are readily obtained (KLM, C. Lee, ADG, data not shown), although most of these mutations have not been characterized.

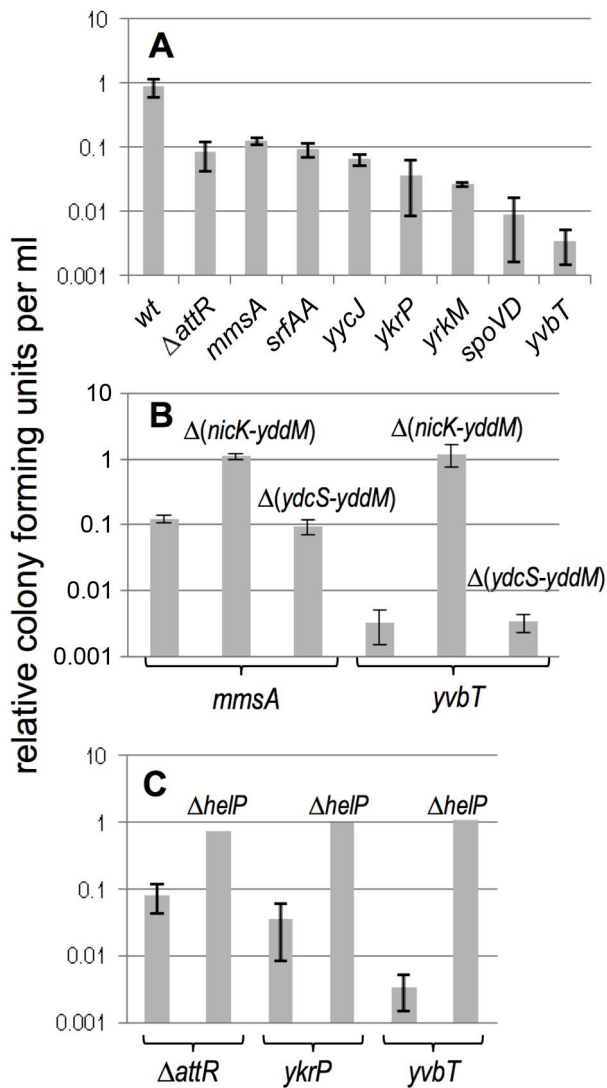


Figure 4. Effects of induction of ICEBs1 gene expression on cell viability. The effects of induction of ICEBs1 gene expression on cell viability are shown for the indicated insertions and their derivatives. Cells were grown in defined minimal medium with arabinose to early exponential phase (OD600~0.05) and xylose was added to induce expression of *P_{xyI}-rapI*, causing induction of ICEBs1 gene expression. The number of colony forming units was measured three hours after induction and compared to cells grown in the absence of xylose (uninduced). All experiments were done at least three times, except for the *helpP* mutants (panel C), which were done twice with similar results. Data presented are averages of the replicates. Error bars represent the standard deviation of at least three replicates. **A.** Drop in viability of strains in which excision of ICEBs1 is defective. Strains used include: wt, that is, *attB::ICEBs1* (CAL874); *attB::ICEBs1 ΔattR::tet* (CAL872); *mmsA::ICEBs1* (KM70); *srlAA::ICEBs1* (KM141); *yycJ::ICEBs1* (KM132); *ykrP::ICEBs1* (KM77); *yrkM::ICEBs1* (KM72); *spoVD::ICEBs1* (KM130); *yvbT::ICEBs1* (KM94). **B.** Data are shown for two secondary insertion sites (*mmsA::ICEBs1* and *yvbT::ICEBs1*). Similar results were obtained with *ykrP::ICEBs1* and *srlAA::ICEBs1* (data not shown). Derivatives of each insertion that delete *nickK* and all downstream ICEBs1 genes ($\Delta(nicK-yddM)$) or that leave *nickK* intact and delete just the downstream genes ($\Delta(ydcS-yddM)$) (Figure 1) were tested. Strains used include: *mmsA::ICEBs1* (KM70); *mmsA::ICEBs1 Δ(nicK-yddM)::cat* (KM366); *mmsA::ICEBs1 Δ(ydcS-yddM)::cat* (KM358); *yvbT::ICEBs1* (KM94); *yvbT::ICEBs1 Δ(nicK-yddM)::cat* (KM369); *yvbT::ICEBs1 Δ(ydcS-yddM)::cat* (KM362). Data for KM70 and KM94 are the same as those shown above in panel A and are shown here for comparison. **C.** The ICEBs1 helicase processivity protein encoded by *helpP* is required for cell killing by ICEBs1. Data are shown for

two secondary integration sites (*ykrP* and *yvbT*) and the excision defective ICEBs1 $\Delta attR$. The *helpP* allele is a non-polar deletion [19]. Strains used include: *attB::ICEBs1 ΔattR::tet* (CAL872); *attB::ICEBs1 ΔhelpP ΔattR::tet* (KM437); *ykrP::ICEBs1* (KM77); *ykrP::ICEBs1 ΔhelpP* (KM429); *yvbT::ICEBs1* (KM94); *yvbT::ICEBs1 ΔhelpP* (KM459). Data for KM94, KM77, and CAL872 are the same as those shown above in panel A and are shown here for comparison. doi:10.1371/journal.pgen.1003623.g004

ICEBs1 replication functions are required for the drop in viability of excision-defective insertions

Because the drop in proliferation and viability in the first few hours after induction of ICEBs1 gene expression occurs in ICEBs1 excision-defective and not in excision-competent strains, the decreased viability is likely due to a cis-acting property of ICEBs1 and not a diffusible ICEBs1 product. One of the more dramatic changes following induction of ICEBs1 gene expression is induction of multiple rounds of unidirectional rolling circle replication [15]. This replication initiates from the ICEBs1 origin of transfer *oriT*, requires the ICEBs1 relaxase encoded by *nickK* and the helicase processivity factor encoded by *helpP* (previously *ydcP*) [19]. Rolling circle replication of ICEBs1 occurs even when ICEBs1 is unable to excise from the chromosome as observed previously for a mutant unable to excise [15]. Therefore, we expected that induction of ICEBs1 gene expression in the secondary site insertions would lead to unidirectional rolling circle replication from *oriT* in the host chromosome (Figure 5). It seemed

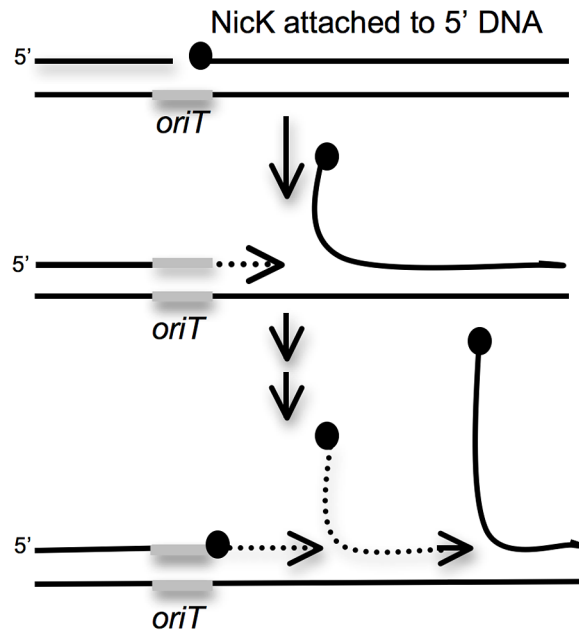


Figure 5. Cartoon of repeated rolling-circle replication from the ICEBs1 *oriT* that is stuck in the chromosome. Rolling circle replication is induced in ICEBs1 insertions that are unable to excise from the chromosome. During this replication, the ICEBs1 relaxase NickK (black circles) nicks a site in *oriT*, the origin of transfer (gray bar) that also functions as an origin of replication [15,23]. NickK presumably becomes covalently attached to the 5' end of the nicked DNA. Replication extends (dotted line with arrow) from the free 3'-end, and regenerates a functional *oriT* that is a substrate for another molecule of NickK. The only other ICEBs1 product needed for ICEBs1 replication is the helicase processivity factor *HelP* [19]. The rest of the replication machinery (not shown) is composed of host-encoded proteins. doi:10.1371/journal.pgen.1003623.g005

likely that this replication could cause damage to the chromosome and lead to the decrease in cell viability.

We tested *nick* and the genes downstream for effects on cell viability following induction of *ICEBs1* gene expression in the excision-defective insertions. Preliminary experiments indicated that loss of *nick* restored viability after induction of *ICEBs1* gene expression. However, this effect could have been due to polarity on downstream genes. Unfortunately, *nick* null mutants are difficult to fully complement [23], perhaps because NicK might act preferentially in cis. In addition, complementation of other supposedly “non-polar” mutations in *ICEBs1* are not complemented fully [19,24]. Therefore, to test if loss of *nick* was responsible for the suppression of lethality, or if the suppression was due to loss of expression of a downstream gene, we compared two different deletions in *ICEBs1*. One deletion removed *nick* and most of the downstream genes $\{\Delta(nick-yddM)\}$ (Figure 1D). In the second deletion, *nick* was intact, but most of the genes downstream from *oriT* and *nick* were removed $\{\Delta(ydcS-yddM)\}$ (Figure 1E).

We found that deletion of *nick* alleviated the growth defect of excision-defective secondary insertions, including *mmsA::ICEBs1* and *yvbT::ICEBs1* that caused the most severe drop in viability (Figure 4B). Deletion of the genes downstream from *nick* did not alleviate the drop in viability (Figure 4B), indicating that expression of these genes (many encoding conjugation functions) was not the cause of the decreased cell viability. In addition, in preliminary experiments, we found that several suppressor mutations that restore viability to an excision-defective *ICEBs1* (in this case, at *attB*) were null mutations in *nick* (C. Lee, ADG, unpublished results). Together, these results indicate that a NicK-dependent process is causing the drop in viability of the excision-defective *ICEBs1*.

NicK creates a nick at a specific site in *ICEBs1 oriT* [23], and nicking is required for *ICEBs1* replication (and conjugation) [15]. To determine if the drop in cell viability was due to nicking per se, or to replication, we used a recently defined *ICEBs1* gene, *helP*, which encodes a helicase processivity factor that is needed for *ICEBs1* replication but not for nicking [19,23]. Deletion of *helP* (Figure 1F) is not polar on *nick* and does not affect nicking at *oriT* [19]. Deletion of *helP* completely alleviated the growth defect associated with induction of *ICEBs1* (Figure 4C).

Based on these results, we conclude that unidirectional rolling circle replication from *oriT* in the chromosome most likely caused the drop in viability of the excision-defective *ICEBs1*. The decrease in viability could be due to breaks and degradation of chromosomal DNA around the site of insertion and/or disruptions in host chromosomal replication caused by the multiple rounds of rolling circle replication from *oriT* (Figure 5).

Induction of the SOS response in strains in which *ICEBs1* is defective in excision

We found that induction of *ICEBs1* gene expression in the excision-defective insertions caused induction of the host SOS response. Like that in other organisms, the SOS response in *B. subtilis* results in increased expression of a large set of genes in response to DNA damage or replication stress [25]. We used a *lacZ* fusion to a damage-inducible gene, *dinC-lacZ* [26,27], to monitor the SOS response in cells following induction of *ICEBs1*. Without induction of *ICEBs1* gene expression, there was no detectable β -galactosidase activity above background levels, indicating that none of the insertions alone caused elevated SOS gene expression. In all of the excision-defective *ICEBs1* strains analyzed (*ICEBs1* $\Delta attR$ in *attB*, and insertions in *mmsA*, *yvbT*, *ykrP*, *stfAA*, and *yrkM*), there was a ≥ 3.5 -fold increase in β -galactosidase levels from the *dinC-lacZ* fusion 3 hrs after induction of *ICEBs1* gene expression

(Figure 6). In contrast, there was no detectable increase in β -galactosidase activity three hrs after induction of *ICEBs1* gene expression in the excision-competent insertion in *attB* (Figure 6). There was no apparent correlation between the amount of SOS induction and the severity of the viability defect. For example, one of the strains with the most severe viability defect (*ICEBs1* in *ydcP*) had a relatively low amount of expression of *dinC-lacZ* (Figure 6). However, the amount of SOS induction could be an underestimate since many cells in the population lose viability.

Induction of *dinC-lacZ* in the strains with *ICEBs1* in secondary attachment sites was consistent with prior preliminary experiments using DNA microarrays that indicated induction of the SOS response in *ICEBs1 int* and *xis* mutants that are incapable of excision (N. Kavanaugh, C. Lee, ADG, unpublished results). Based on these results, we conclude that induction of *ICEBs1* gene expression in cells in which *ICEBs1* is stuck in the chromosome causes DNA damage that induces the host SOS response. However, the SOS response per se is not what caused cell death.

Discussion

We isolated and characterized insertions of the integrative and conjugative element *ICEBs1* of *B. subtilis* into secondary integration (attachment or insertion) sites. Secondary integration sites appear to be used naturally, even in the presence of the primary site, at a frequency of $\sim 10^{-4}$ to 10^{-3} of that of the primary site, indicating that approximately 100–1,000 cells in a population of $\sim 10^6$ transconjugants will have *ICEBs1* at a secondary site. We found that insertions in secondary sites are detrimental for the propagation of *ICEBs1* and detrimental to the survival of the host cells. These detrimental effects likely provide selective pressure to maintain the already established site-specificity. Below we discuss target site selection among ICEs, aspects of *ICEBs1* biology that make insertions into secondary sites detrimental, and the more general implications for the evolution of ICEs.

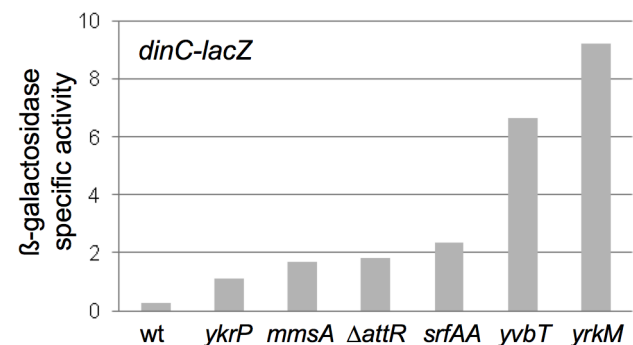


Figure 6. Induction of the SOS response. The β -galactosidase specific activities from the SOS transcriptional reporter fusion *dinC-lacZ* in strains with *ICEBs1* in the indicated secondary attachment sites are presented. Strains were grown as described in Figure 4 and samples for β -galactosidase assays were taken 3 hours after induction of *ICEBs1* gene expression. Data presented are the averages of two biological replicates (four for $\Delta attR$ strain KM392). For all of the strains with insertions in secondary attachment sites, the values from the biological replicates were within 20% of the average. Strains used include: wt, *attB::ICEBs1* (KM390); *ykrP::ICEBs1* (KM402); *mmsA::ICEBs1* (KM394); *attB::ICEBs1* $\Delta attR::tet$ (KM392); *srfAA::ICEBs1* (KM400); *yvbT::ICEBs1* (KM396); *yrkM::ICEBs1* (KM404).

doi:10.1371/journal.pgen.1003623.g006

Target site selection and maintenance of tRNA genes as integration sites

We have identified 15 different secondary insertion sites for *ICEBsI*. Some of these sites are similar to the primary attachment site, but some are quite different. Based on the diversity of sites, and the isolation of only a single insertion in many of them, it is likely that we are nowhere near saturation for identifying all possible sites in non-essential regions. Given that there is some sequence conservation among the secondary sites, DNA sequence is clearly important in the potential function as an integration site. However, we suspect that other factors also contribute. These factors could include possible roles for nucleoid binding proteins, other DNA binding proteins, transcription, and local supercoiling.

Many site-specific ICEs have preferred integration sites in tRNA genes. This preference is thought to occur, at least in part, because tRNA genes are highly conserved and contain inverted repeats that are typically used as integration targets for site-specific recombinases [9]. We postulate that the selective pressure to maintain site-specific integration in a tRNA gene comes from a combination of factors, including: the conservation of tRNAs, the ability of an ICE to efficiently excise from the primary attachment site, and the decreased cell viability and decreased ability of an ICE to spread when excision is reduced due to integration into a secondary site.

Selective pressures against ICEs in secondary attachment sites

Our results indicate that there are at least two main types of selective pressures against propagation of *ICEBsI* that has inserted into a secondary integration site. First, there is strong pressure against the spread of that particular element due to the large defect in its ability to excise and the instability of circular *ICEBsI* when it forms a heteroduplex. The excised circular form of an ICE is necessary for its complete transfer to a recipient cell. At least one other ICE has a reduced excision frequency from a secondary integration site. Excision of SXT from a secondary attachment site in *Vibrio cholerae* was reduced 3–4-fold relative to its ability to excise from the primary attachment site [28]. In addition, lysogenic phages can also have reduced excision efficiencies from secondary attachment sites [29]. Insertion of any type of mobile genetic element into a location from which it has trouble getting out will be deleterious to the further horizontal propagation of that element. Based on our results, this is particularly true for *ICEBsI*.

In addition to the defect in *ICEBsI* excision and transfer from secondary integration sites, there is a decrease in cell viability following induction of *ICEBsI* gene expression. *ICEBsI* gene expression is normally induced under conditions of starvation or cell crowding when the activator RapI is expressed and active, or when the RecA-dependent SOS response is induced [22]. Induction of *ICEBsI* gene expression causes rolling circle replication from the *ICEBsI* origin of transfer *oriT* [15,19]. Our results indicate that rolling circle replication from an element that is unable to efficiently excise from the chromosome causes a drop in cell viability. This drop is likely due to chromosomal damage and stalling of the chromosomal replication forks when they reach the complex structure formed by repeated initiation of rolling circle replication from *oriT* in the chromosome (Figure 5).

We suspect that autonomous replication is a common property of many ICEs but has not been generally observed because of the low frequency of induction and excision of most of these elements. There are indications that some other ICEs undergo autonomous replication [1,16–18]. If autonomous replication of ICEs is widespread, as we postulate [15,19], then there should be selective

pressure against viability of cells in which an ICE is induced, replicates, and is unable to excise.

There were at least two different effects caused by replication of excision-defective elements. Replication from *ICEBsI* in the chromosome caused a drop in cell viability of at least 10-fold, but sometimes caused a severe drop, 100–1000-fold in about 3 hrs. We do not know what causes this severe drop in viability, but it requires active replication of the *ICEBsI* that is unable to excise from a specific chromosomal location. This severe drop in viability could be due to increased dosage of nearby genes or perhaps differential fragility of these chromosomal regions. In any case, the severe drop in viability provides even stronger selective pressure against propagation of the strains with insertions of *ICEBsI* in these locations.

The growth defect associated with the secondary insertions is most obvious when *ICEBsI* gene expression is induced. Cells with *ICEBsI* insertions in secondary attachment sites might be purged from the population under natural conditions of induction, providing selective pressure against maintenance of integrants in secondary sites and favoring a site-specific strategy of integration and excision.

We estimated the effects of insertions in secondary sites in populations without experimentally induced activation of *ICEBsI*. The “spontaneous” activation and excision frequency of *ICEBsI* in a population of cells is estimated to be approximately one cell in 10^4 – 10^5 [10,22,30]. Assuming a frequency of activation of *ICEBsI* of $\sim 10^{-4}$ per generation, and that all activated cells with *ICEBsI* in a secondary site die, we estimate that it would take $\sim 23,000$ generations for a population of cells with *ICEBsI* in a secondary site to be 0.1 times the size of a population of cells with *ICEBsI* in the primary site. The activation frequency increases under several conditions likely to be more relevant than growth in the lab, including: the presence of cells without *ICEBsI*, entry into stationary phase, and during the SOS response [10,11,22]. For example, if activation of *ICEBsI* actually occurs in 0.1% of cells, then it would take $\sim 2,300$ generations for the secondary site insertion population to be 0.1 times the population of cells with *ICEBsI* in the primary site. These effects are difficult to measure experimentally, but easy to see when *ICEBsI* is efficiently induced.

ICEs with single versus multiple integration sites

ICEs of the Tn916/Tn1545 family can integrate into multiple sites in many organisms, yet they are not known to cause a defect in cell growth when gene expression is induced. Tn916 and most family members contain *tetM*, a gene encoding resistance to tetracycline. Expression of *tetM* and Tn916 genes is induced in the presence of tetracycline [31]. Tn916 has two *helP* (helicase processivity) homologues and we predict that it undergoes autonomous rolling circle replication [19]. Despite relatively low excision frequencies, tetracycline-induced Tn916 gene expression is not known to cause a drop in cell viability. Tetracycline induces expression of several Tn916 genes, including those needed for excision. However, the Tn916 relaxase (*orf20*), the two *helP* homologues (*orf22* and *orf23*), and the conjugation genes are not expressed until Tn916 excises and circularizes [31]. Based on analogy to *ICEBsI*, we have postulated that Tn916 is capable of autonomous rolling circle replication [15] and that the relaxase (*orf20*) and at least one of the *helP* homologues are likely needed for this replication [19]. The regulation of Tn916 gene expression specifically prevents expression of these putative replication functions until after excision. Consequently, rolling circle replication of Tn916 cannot occur while the element is integrated in the chromosome. We speculate that some of the evolutionary pressures to establish and maintain a high degree of site specificity

is lost when expression of ICE replication functions does not occur until after excision from the host genome.

Materials and Methods

Media and growth conditions

Bacillus subtilis was grown at 37°C in LB or defined S7₅₀ minimal medium with arabinose (1%) as carbon source. Antibiotics and other chemicals were used at the following concentrations: isopropyl β-D-1-thiogalactopyranoside (IPTG) (1 mM), chloramphenicol (*cat*, 5 μg/ml), kanamycin (*kan*, 5 μg/ml), spectinomycin (*spc*, 100 μg/ml), erythromycin (0.5 μg/ml) and lincomycin (12.5 μg/ml) together, to select for macrolide-lincosamide-streptogramin B resistance (*mls* or *erm*).

Bacillus subtilis strains and alleles

B. subtilis strains used are listed in Table 2. All except BTS14 are derived from AG174 (JH642) and contain mutations in *trpC* and *pheA* (not shown). Most of the strains were constructed using natural transformation or conjugation, as described below. Many alleles were previously described. *dinC18::Tn917lac* is an insertion in the damage-inducible gene *dinC* and creates a transcriptional fusion to *lacZ* [27]. Most ICEBs1 strains contained a kanamycin-resistance cassette { $\Delta(\text{rapI-phrI})342::kan$ } [11]. ICEBs1 was induced by overexpression of *rapI* from a xylose-inducible promoter using *amyE::*{(P_{xyl}-*rapI*), *spc*} [24] or from an IPTG-inducible promoter using *amyE::*{(P_{spank(hy)}-*rapI*), *spc*} [11]. $\Delta attR100::tet$ deletes 216 bp spanning the junction between the right end of ICEBs1 and the chromosome [10]. $\Delta helP155$ is an unmarked 413-bp deletion that removes the entire coding sequence and the 35 bp *helP-ydcQ* intergenic region (Figure 1F) [19].

$\Delta attB$ mutant with a compensatory mutation in *trnS-leu1*. $\Delta attB::cat$ is a deletion-insertion that is missing ICEBs1 and removes 185 bp that normally contains the primary chromosomal ICEBs1 attachment site, resulting in the loss of a functional *trnS-leu2* [10]. Although *trnS-leu2* is non-essential [10,32], cells with $\Delta attB$ do not grow as well as wild type. To improve the growth of $\Delta attB::cat$, we used a compensatory mutation in *trnS-leu1* that changes the anti-codon to that normally found in *trnS-leu2* (C. Lee, & ADG), analogous to the *leuF1* mutation previously described [32]. The compensatory mutation was constructed by site-directed mutagenesis using the overlap-extension PCR method [33]. Because *trnS-leu1* and $\Delta attB::cat$ are genetically linked, we selected for chloramphenicol resistant colonies and screened for the single bp mutation in *trnS-leu1* by sequencing. In addition to the mutant *trnS-leu1* allele (*trnS-leu1-522*), the strain had an additional mutation, (5'-CAAAAAAACTAAA to 5'-CAAAAAAACTAAG) in the non-coding region between $\Delta attB::cat$ and *yddN*. Growth of the resulting strain, CAL522, was indistinguishable from that of wild type. This strain stably acquired ICEBs1 in conjugation experiments at a frequency ~0.5% of that of wild type, approximately 10-fold lower than the strain without the compensatory mutation in *trnS-leu1* [10]. We do not understand the cause of this reproducible difference.

Deletion of *nicK* and downstream genes. We constructed two large deletion-insertion mutations in ICEBs1, one removing *nicK* and all downstream genes, $\Delta(nicK-yddM)::cat$, and the other leaving *nicK* intact, but removing the downstream genes, $\Delta(ydcS-yddM)::cat$. Both deletions leave the ends of ICEBs1 intact (Figure 1D, E), have *cat* (chloramphenicol resistance) from pGEMcat [34], and were constructed using long-flanking homology PCR [35]. The $\Delta(nicK-yddM)::cat$ allele contains the first 127 bp in the 5' end of *nicK*. The $\Delta(ydcS-yddM)::cat$ allele contains the first 29 bp in the 5' end of *ydcS*. Both deletions

(Figure 1) extend through the first 170 bp in *yddM*. The alleles were first transformed into wild type strain AG174. Chromosomal DNA was then used to transfer the alleles into other strains, including KM70 (*mmsA::ICEBs1*), KM94 (*yvbT::ICEBs1*), KM77 (*ykrP::ICEBs1*), KM141 (*stfAA::ICEBs1*), and CAL874 (*ICEBs1* at *attB*). In all cases, the incoming deletion associated with *cat* replaced the $\Delta(\text{rapI-phrI})342::kan$ allele present in ICEBs1 in the recipient.

Deletion of *yvbT* in *mmsA::ICEBs1*. We constructed a deletion-insertion that removes the 19 bases before *yvbT* and the first 808 bp of *yvbT*, leaving the last 200 bp intact. The sequence from *yvbT* was replaced with *cat*, from pGEMcat [34], using long-flanking homology PCR [35]. The insertion-deletion was verified by PCR and the mutation was introduced into strain KM70 (*mmsA::ICEBs1*) by transformation.

Isolation and identification of secondary ICEBs1 integration sites

Mating ICEBs1 into a $\Delta attB$ recipient. Mating assays were performed essentially as described [10,11]. Excision of a kanamycin resistant ICEBs1 (*ICEBs1* $\Delta(\text{rapI-phrI})342::kan$) was induced in the donor cells by overproduction of RapI from P_{spank(hy)}-*rapI*. Donors (resistant to kanamycin and spectinomycin) were mixed with an approximately equal number of recipients (resistant to chloramphenicol) and filtered on sterile cellulose nitrate membrane filters (0.2 μm pore size). Filters were cut into 8 pieces (so that transconjugants were independent isolates), placed on Petri plates containing LB and 1.5% agar, and incubated at 37°C for 3 hours. Cells from each piece of filter were streaked for independent transconjugants by selecting for the antibiotic resistance conferred by the incoming ICEBs1 (kanamycin) and the resistance unique to the recipient (chloramphenicol). The recipient used in this report { $\Delta attB::cat$ *trnS-leu1-522*} is different from the recipient { $\Delta attB::cat$ } used previously [10]. The *trnS-leu1-522* confers normal growth to the $\Delta attB$ ($\Delta trnS-leu2$) mutant (see above).

Inverse PCR to identify the site of insertion of independent transconjugants. Identification of integration sites was done essentially as described previously [10]. Briefly, we used inverse PCR to amplify the junction between the chromosome and the right (*yddM*) end of ICEBs1 integrated into various secondary sites. Chromosomal DNA was digested with HindIII and approximately 50 ng was ligated in a 100 μl reaction to favor circularization of DNA fragments. One-fourth of the ligation reaction was used in inverse PCR with either of two primer pairs (CLO17-CLO58 or CLO50-qJMA97) designed to amplify the ICEBs1 and chromosomal sequences flanking *yddM*. PCR products were sequenced with primers CLO17, CLO50, qJMA207, and CLO114 (primers are described in Table 3). Comparison to the *B. subtilis* genome sequence indicated where ICEBs1 had integrated.

Backcross of ICEBs1 insertions. Seven of the 15 different insertions of ICEBs1 in secondary attachment sites were initially chosen for further study. These were first backcrossed into a strain cured of ICEBs1 (JMA222). P_{xyl}-*rapI* (*amyE::*{(P_{xyl}-*rapI*) *spc*}) was introduced into these strains by transformation and selection for spectinomycin resistance using chromosomal DNA from strain MMB869. We verified that ICEBs1 was still at the original secondary attachment site using PCR with site-specific primers. The final strains from these crosses include: KM70 (*mmsA::ICEBs1*), KM94 (*yvbT::ICEBs1*), KM72 (*ykrM::ICEBs1*), KM77 (*ykrP::ICEBs1*), KM130 (*spoVD::ICEBs1*), KM141 (*stfAA::ICEBs1*), and KM132 (*yycJ::ICEBs1*).

Table 2. *B. subtilis* strains used.

Strain	relevant genotype (comment and/or reference)
AG174	<i>phe trp</i> [39]
AG1624	<i>zjb-82::Tn917</i> (insertion at 65°) [40]
BTS13	PY79 (<i>trp⁺ phe⁺</i>) Δ mutSL::spc [41]
CAL522	<i>trnS-leu1-522</i> Δ attB::cat
CAL572	<i>yomR572::(ICEBs1 Δ(rapI-phrI)342::kan) ΔattB::cat comK::cat::spc</i> [10]
CAL575	<i>yvbT575::(ICEBs1 Δ(rapI-phrI)342::kan) ΔattB::cat comK::cat::spc</i> [10]
CAL576	<i>yqhG576::(ICEBs1 Δ(rapI-phrI)342::kan) ΔattB::cat comK::cat::spc</i> [10]
CAL577	<i>yobJ577::(ICEBs1 Δ(rapI-phrI)342::kan) ΔattB::cat comK::cat::spc</i> [10]
CAL578	Intergenic <i>ygxA rrmD-16S-578::(ICEBs1 Δ(rapI-phrI)342::kan) ΔattB::cat comK::cat::spc</i> [10]
CAL872	Δ attR100::tet Δ (rapI-phrI)342::kan <i>amyE::(Pxyl-rapI) spc</i>
CAL874	Δ (rapI-phrI)342::kan <i>amyE::(Pxyl-rapI) spc</i> [15]
JMA168	Δ (rapI-phrI)342::kan <i>amyE::(Pspank(hy)-rapI) spc</i> [23]
J3	<i>srfAA3::(ICEBs1 Δ(rapI-phrI)342::kan) trnS-leu1-522 ΔattB::cat</i>
J4	<i>yycJ4::(ICEBs1 Δ(rapI-phrI)342::kan) trnS-leu1-522 ΔattB::cat</i>
J9	<i>yrkM9::(ICEBs1 Δ(rapI-phrI)342::kan) trnS-leu1-522 ΔattB::cat</i>
J11	<i>yqhG11::(ICEBs1 Δ(rapI-phrI)342::kan) trnS-leu1-522 ΔattB::cat</i>
J12	<i>yisQ12::(ICEBs1 Δ(rapI-phrI)342::kan) trnS-leu1-522 ΔattB::cat</i>
J14	<i>mmsA14::(ICEBs1 Δ(rapI-phrI)342::kan) trnS-leu1-522 ΔattB::cat</i>
J16	<i>ykrP16::(ICEBs1 Δ(rapI-phrI)342::kan) trnS-leu1-522 ΔattB::cat</i>
JMA222	ICEBs1 ⁰ /cured of ICEBs1 [11]
KI1254	<i>dinC18::Tn917lac</i> ; allele originally from YB5018 [27]
KM5	<i>yghL5::(ICEBs1 Δ(rapI-phrI)342::kan) trnS-leu1-522 ΔattB::cat</i>
KM8	<i>spoVD8::(ICEBs1 Δ(rapI-phrI)342::kan) trnS-leu1-522 ΔattB::cat</i>
KM10	<i>ydbJ10::(ICEBs1 Δ(rapI-phrI)342::kan) trnS-leu1-522 ΔattB::cat</i>
KM70	<i>mmsA15::(ICEBs1 Δ(rapI-phrI)342::kan) amyE::(Pxyl-rapI) spc</i>
KM72	<i>yrkM9(J9)::(ICEBs1 Δ(rapI-phrI)342::kan) amyE::(Pxyl-rapI) spc</i>
KM77	<i>ykrP16::(ICEBs1 Δ(rapI-phrI)342::kan) amyE::(Pxyl-rapI) spc</i>
KM94	<i>yvbT575::(ICEBs1 Δ(rapI-phrI)342::kan) amyE::(Pxyl-rapI) spc</i>
KM110	ICEBs1 ⁰ <i>zjb-82::Tn917</i> (insertion at 65°)
KM111	ICEBs1 ⁰ <i>zjb-82::Tn917 trnS-leu1-522 ΔattB::cat</i>
KM130	<i>spoVD8::(ICEBs1 Δ(rapI-phrI)342::kan) amyE::(Pxyl-rapI) spc</i>
KM132	<i>yycJ4::(ICEBs1 Δ(rapI-phrI)342::kan) amyE::(Pxyl-rapI) spc</i>
KM141	<i>srfAA3::(ICEBs1 Δ(rapI-phrI)342::kan) amyE::(Pxyl-rapI) spc</i>
KM250	ICEBs1 Δ (rapI-phrI)342::kan <i>amyE::(Pxyl-rapI) cat</i>
KM252	<i>mmsA15::(ICEBs1 Δ(rapI-phrI)342::kan) amyE::(Pxyl-rapI) cat</i>
KM268	<i>mmsA15::(ICEBs1 Δ(rapI-phrI)342::kan) amyE::(Pxyl-rapI) cat ΔmutSL::spc</i>
KM304	<i>mmsA15::(ICEBs1 Δ(rapI-phrI)342::kan) amyE::(Pxyl-rapI) spc ΔyvbT::cat</i>
KM358	<i>mmsA15::(ICEBs1 Δ(ydcS-yddM)356::cat) amyE::(Pxyl-rapI) spc</i>
KM362	<i>yvbT575::(ICEBs1 Δ(ydcS-yddM)356::cat) amyE::(Pxyl-rapI) spc</i>
KM366	<i>mmsA15::(ICEBs1 Δ(nick-yddM)354::cat) amyE::(Pxyl-rapI) spc</i>
KM369	<i>yvbT575::(ICEBs1 Δ(nick-yddM)354::cat) amyE::(Pxyl-rapI) spc</i>
KM384	<i>srfAA3::(ICEBs1 Δ(ydcS-yddM)356::cat) amyE::(Pxyl-rapI) spc</i>
KM386	<i>srfAA3::(ICEBs1 Δ(nick-yddM)354::cat) amyE::(Pxyl-rapI) spc</i>
KM388	<i>ykrP16::(ICEBs1 Δ(ydcS-yddM)356::cat) amyE::(Pxyl-rapI) spc</i>
KM389	<i>ykrP16::(ICEBs1 Δ(nick-yddM)354::cat) amyE::(Pxyl-rapI) spc</i>
KM390	Δ (rapI-phrI)342::kan <i>amyE::(Pxyl-rapI) spc dinC18::Tn917(lacZ mls)</i>
KM392	Δ attR100::tet Δ (rapI-phrI)342::kan <i>amyE::(Pxyl-rapI) spc dinC18::Tn917lac</i>
KM394	<i>mmsA15::(ICEBs1 Δ(rapI-phrI)342::kan) amyE::(Pxyl-rapI) spc dinC18::Tn917lac</i>
KM396	<i>yvbT575::(ICEBs1 Δ(rapI-phrI)342::kan) amyE::(Pxyl-rapI) spc dinC18::Tn917lac</i>

Table 2. Cont.

Strain	relevant genotype (comment and/or reference)
KM400	<i>srfAA3::(ICEBs1 Δ(rapl-phr)342::kan amyE::(Pxyl-<i>rapI</i>) spc) dinC18::Tn917lac</i>
KM402	<i>ykrP16::(ICEBs1 Δ(rapl-phr)342::kan amyE::(Pxyl-<i>rapI</i>) spc) dinC18::Tn917lac</i>
KM404	<i>yrkM9(J9)::(ICEBs1 Δ(rapl-phr)342::kan amyE::(Pxyl-<i>rapI</i>) spc) dinC18::Tn917lac</i>
KM429	<i>ykrP16::(ICEBs1 Δ<i>help</i> Δ(rapl-phr)342::kan amyE::(Pxyl-<i>rapI</i>) spc)</i>
KM437	<i>ΔattR100::tet Δ<i>help</i> Δ(rapl-phr)342::kan amyE::(Pxyl-<i>rapI</i>) spc</i>
KM524	<i>ICEBs1⁰ (attB⁺) amyE::(lacZ, <i>mls</i>); used as recipient in conjugation to detect insertions in secondary sites</i>
KM459	<i>yvbT575::(ICEBs1 Δ<i>help</i> Δ(rapl-phr)342::kan amyE::(Pxyl-<i>rapI</i>) spc)</i>
MMB868	<i>amyE::(Pxyl-<i>rapI</i>) cat</i>
MMB869	<i>amyE::(Pxyl-<i>rapI</i>) spc</i> [30]
REM54	<i>ΔattB::cat</i> [10]

doi:10.1371/journal.pgen.1003623.t002

Assays for excision and integration of ICEBs1

Detecting excision from secondary insertions. Excision of ICEBs1 from a chromosomal attachment site creates an extrachromosomal ICEBs1 circle and an “empty” attachment site (also called “repaired chromosomal junction”). Each product was measured using specific primers for quantitative real time PCR (qPCR), using a LightCycler 480 Real-Time PCR system with Syber Green detection reagents (Roche), essentially as described [15]. Cells were grown in defined minimal medium with arabinose as carbon source. Products from excision were determined two hours after addition of xylose to induce expression of Pxyl-*rapI* to cause induction of ICEBs1 gene expression.

The amount of each empty attachment site was compared to a chromosomal reference gene, *cotF*, measured with primers CLO257-CLO258. The amount of empty attachment site from each of the secondary sites was normalized to strain JMA222, an ICEBs1-cured strain that simulates 100% excision. Standard curves for qPCR with *cotF* and the repaired junction for each secondary insertion were generated using genomic DNA from JMA222. Primers (in parentheses) for empty secondary attachment sites were specific for: *yrkM* (CLO117-ABO17), *mmsA* (CLO109-ABO18), *yyeJ* (KM18-KM19), *stfAA* (KM22-KM23), *spoVD* (KM20-KM21), *yvbT* (ABO14-ABO15), *ykrP* (KM154-KM16), and *attB* (CLO261-CLO262).

The amount of ICEBs1 circle that forms after excision from the chromosome was measured with primers AB019-CLO114. The amount of excised circle was compared to the chromosomal reference *cotF* (primers CLO257-CLO258), and normalized to the amount of excised circle from *attB* (strain CAL874). Standard curves for qPCR for *cotF* and the excised circle were generated using genomic DNA from RapI-induced CAL874. Primer sequences are presented in Table 3.

Detecting integration at *yrkM* in a pool of transconjugants. ICEBs1 was transferred from donor strain KM250 to recipient KM524 by conjugation, selecting for resistance to kanamycin and MLS antibiotics. Approximately 10⁸ transconjugants were collected from four separate conjugation experiments (done on filters placed on agar plates). Cells were washed off of all four filters with a total of 10 ml of minimal salts and aliquots of 0.2 ml were spread on selective plates to give ~2×10⁶ transconjugants per plate. After overnight growth, plates (~50) with the transconjugants were flooded with minimal salts, cells were scraped, collected, and transconjugants from all plates were pooled.

DNA was isolated from the pool of transconjugants and used as a template for qPCR with primers to detect the junction between

yrkM and ICEBs1 (primers CLO116 and KM76). Values from this qPCR were compared to qPCR values for a reference gene (*cotF*). Values were normalized to a strain (KM72) that contains *yrkM::ICEBs1* and represents 100% integration at *yrkM*. Values for *yrkM::ICEBs1* in the pool of transconjugants were in the linear range of the qPCR and ≥3-fold above the background signal from the negative control (JMA222, which is cured of ICEBs1). DNA used for standard curves was from strain KM72 (*yrkM::ICEBs1*). The frequency of integration at *attB* was determined by qPCR with primers CLO273 and CLO264. Values were compared to *cotF* and normalized to a strain with ICEBs1 at *attB* (strain AG174 or CAL874). DNA used for standard curves was from AG174 or CAL874. The entire experiment was done twice with similar results.

Detecting integration at secondary sites after mating from a secondary site. Independent transconjugants, from donors with ICEBs1 at secondary attachment sites, were analyzed for the location of ICEBs1. Sites analyzed and primers used included: *yrkM* (CLO116-CLO17 or oJMA141-CLO17); *mmsA* (CLO109-oJMA141); *yyeJ* (CLO17-KM4); *stfAA* (oJMA141-KM5); and *attB* (CLO17-oJMA100). The presence of ICEBs1 in the transconjugants was verified using primers internal to ICEBs1 (oJMA102-oJMA22).

Cell viability assays

Strains were grown in defined minimal medium with arabinose and expression of Pxyl-*rapI* was induced with 1% xylose at OD600 of 0.05. The number of colony forming units (CFU) was determined 3 hours after addition of xylose. For each strain, the number of CFU/ml 3 hrs after expression of Pxyl-*rapI* was compared to the number of CFU/ml without expression of Pxyl-*rapI*. All experiments were done at least twice.

β-galactosidase assays

Cells were grown and treated as described for viability assays. Samples were taken 3 hours after induction of Pxyl-*rapI*. All experiments were done at least twice. β-galactosidase assays were done essentially as described [36,37]. Specific activity is expressed as the (ΔA420 per min per ml of culture per OD600 unit)×1000.

Modeling competition between cells with ICEBs1 in the primary attachment site versus cells with ICEBs1 in a secondary attachment site

We calculated the predicted population size P after G generations for cells in which ICEBs1 is integrated into a

Table 3. Primers used.

Name	Sequence ¹	Location, use, reference ²
ABO14	CCAACGCAAGATACCTTGC	5' <i>yvbT</i> ; qPCR
ABO15	TGTTCAAGCCAGTAACG	3' <i>yvbT</i> ; qPCR
ABO17	CTGACATATACCACGCCAC	5' <i>yrkM</i> ; qPCR
ABO18	AAACGCAATCCGCTACTTCC	5' <i>mmsA</i> ; qPCR
ABO19	GTATCATTGATGCGGCCAG	near left end of <i>ICEBs1</i> , 3' in <i>trnS-leu2</i> ; qPCR to detect <i>ICEBs1</i> circle or left junction in chromosome
CLO109	GATATCTTGCCGTCACT	3' <i>mmsA</i> ; qPCR
CLO114	CTTAATGCTATAATAAAGGCTTTTG	in <i>ICEBs1</i> , near and extending towards the right end, in same direction as transcription of <i>trnS-leu2</i> ; PCR, qPCR, sequencing
CLO116	CGCAGAGAGTTGCTGGTAAAC	just upstream of <i>yrkM</i> (35 codons), in same direction as transcription of <i>yrkM</i> (5'); qPCR, PCR
CLO117	TGTAGAGTTCCTGGCCTCT	just downstream of <i>yrkM</i> , in opposite direction of transcription of <i>yrkM</i> (3'); qPCR, PCR
CLO17	CCATTTACTGCCAGAATAAATAACAATCATG	in <i>ICEBs1</i> , near and extending towards the right end, in same direction as transcription of <i>trnS-leu2</i> [10]; ~50 bp farther from the right end of <i>ICEBs1</i> than CLO114; PCR, qPCR, sequencing
CLO257	GGATGAACGCAGAACATTGG	5' <i>cotF</i> , chromosomal gene for reference; qPCR
CLO258	GCTCAACCCCTGAATAGAC	3' <i>cotF</i> , chromosomal gene for reference; qPCR
CLO261	GCCTACTAAACAGCACAAAC	5', just upstream of <i>trnS-leu2</i> ; qPCR [15,30]
CLO262	AGCAAGTCTTCCCATAGC	3', just outside the right end of <i>ICEBs1</i> ; qPCR [15,30]
CLO264	TATTGAGATGCGGCCGAGAG	3' <i>trnS-leu2</i> , downstream from <i>attB</i> ; qPCR, to detect integration of <i>ICEBs1</i> in <i>attB</i>
CLO273	AGGGCGAACTATGAGTTTGC	near and extending towards right end of <i>ICEBs1</i> ; qPCR, to detect integration of <i>ICEBs1</i> in <i>attB</i>
CLO50	GCCTTCTGCGTCCGGTCG	In <i>kan</i> ; near right end of <i>ICEBs1 Δ(rapl-phr1)::kan</i> ; inverse PCR, sequencing [10]
CLO58	CGCGGATCCGACTGTACCGTACGTTTTAAAGATGATGTAAC	in <i>yddM</i> ; inverse PCR, sequencing [10]
KM15	AGTCCGCTTACCAGGGTAAC	qPCR; 3' <i>ykrP</i> ; qPCR
KM16	GAGCTTGTCACGGACATTCG	qPCR; 5' <i>ykrP</i> ; qPCR
KM18	TATACAGCAAAGCGGAGTG	qPCR; 3' <i>yycJ</i> ; qPCR
KM19	ATGTCATTGGCGATGAGACG	qPCR; 5' <i>yycJ</i> ; qPCR
KM20	GAATTAGCGGAGCGCTTAGG	qPCR; 5' <i>spoVD</i> ; qPCR
KM21	CTGTCCGAAAGCCGTAGTTG	qPCR; 3' <i>spoVD</i> ; qPCR
KM22	GCTCCGATGGTCTATCGTG	qPCR; 5' <i>srfAA</i> ; qPCR
KM23	TTGCAAACGCTCCGCTTCTC	qPCR; 3' <i>srfAA</i> ; qPCR
KM4	CGGACTTGATGTTGAATCGTTGGCGTTTCCC	5' <i>yycJ</i> ; PCR
KM5	GGAGAATACAAAGCGCCGACGACCATGG	5' <i>srfAA</i> ; PCR
KM76	AAAGGCTTTGTAATAAAG	In <i>ICEBs1</i> near and amplifies towards the right end; qPCR
oJMA100	GGGTATACAATCATGGGTATCGAG	in <i>yddN</i> , outside, but near and amplifies towards the right end of <i>ICEBs1</i> ; PCR [10,11,22]
oJMA102	TAATCTAAGCTTCACTCCTCGTTAACTCAACTC	In <i>ICEBs1</i> in <i>xis</i> , amplifies towards the left end of <i>ICEBs1</i> ; PCR [22]
oJMA141	CTTACTTTAGGTAAGTGGGCGAGTTTGTTGG	Overlaps the 3' end of <i>int</i> in <i>ICEBs1</i> ; amplifies toward <i>attL</i> (into <i>trnS-leu2</i>); PCR [10]
oJMA207	GGATGAATTGTTTTAGTACCTAGATTTAGATGTC	In <i>kan</i> ; near right end of <i>ICEBs1 Δ(rapl-phr1)::kan</i> ; amplifies toward left end of <i>ICEBs1</i> ; inverse PCR, sequencing
oJMA227	ATATAAGCTTGCTAGGCTCATTITTTATCATC	in <i>ICEBs1</i> , upstream of <i>ycdN</i> ; amplifies toward the left end of <i>ICEBs1</i> ; PCR
oJMA97	CTGTAAATTATGAATCTCAGATTGTAATCTCTGC	in <i>ICEBs1</i> in <i>yddM</i> , amplifies toward right end of <i>ICEBs1</i> ; inverse PCR [10,11,22]

¹sequences are indicated 5' to 3'.

²the relevant location of each primer is indicated, along with how the primer was used. Primers to chromosomal regions are usually near the site of integration of *ICEBs1*. The position, 5' or 3', in the indicated gene is relative to the direction of transcription of that gene, 5' indicating extension in the same and 3' indicating extension in the opposite direction as transcription. Left and right ends of *ICEBs1* are as in Figure 1.

doi:10.1371/journal.pgen.1003623.t003

secondary attachment site, with an estimated fraction of dead cells, *D*. The estimate of dead cells is based on the fraction of cells in which *ICEBs1* is excised during exponential growth, determined previously to be between 10⁻⁵ to 10⁻⁴. Population size

$P = P_0 \cdot 2^G \cdot (1 - D)^G$, where *P*₀ is the initial population size. The ratio *R* of the number of cells with *ICEBs1* at *attB* to the number of cells with *ICEBs1* in a secondary site is given by $R = P_0 \cdot 2^G$ (for *ICEBs1* in *attB* and assuming no killing upon induction)/

$P_0 \cdot 2^G \cdot (1-D)^G$ (for *ICEBs1* in a secondary site). This equation reduces to $R = 1/(1-D)^G$. This gives $G = \{\log(1/R)\}/\log(1-D)$. For the number of cells with *ICEBs1* in *attB* to be 10-fold greater than the number of cells with *ICEBs1* in a secondary site ($R = 10$) and if the frequency of death is $\sim 10^{-4}$ for the secondary site insertions, then the number of generations to achieve $R = 10$ is: $G = \log(0.1)/\log(0.9999)$ which is $\sim 23,000$.

Acknowledgments

We thank J. Wilks for preliminary isolation of some of the insertions in secondary attachment sites, C. Lee for helpful discussions and construction

References

- Wozniak RA, Waldor MK (2010) Integrative and conjugative elements: mosaic mobile genetic elements enabling dynamic lateral gene flow. *Nat Rev Microbiol* 8: 552–563.
- Guglielmini J, Quintais L, Garcillan-Barcia MP, de la Cruz F, Rocha EP (2011) The repertoire of ICE in prokaryotes underscores the unity, diversity, and ubiquity of conjugation. *PLoS Genet* 7: e1002222.
- Lee CA, Thomas J, Grossman AD (2012) The *Bacillus subtilis* conjugative transposon *ICEBs1* mobilizes plasmids lacking dedicated mobilization functions. *J Bacteriol* 194: 3165–3172.
- Salyers AA, Shoemaker NB, Stevens AM, Li LY (1995) Conjugative transposons: an unusual and diverse set of integrated gene transfer elements. *Microbiol Rev* 59: 579–590.
- Hochhut B, Waldor MK (1999) Site-specific integration of the conjugal *Vibrio cholerae* SXT element into *pfkC*. *Mol Microbiol* 32: 99–110.
- Roberts AP, Mullany P (2009) A modular master on the move: the Tn916 family of mobile genetic elements. *Trends Microbiol* 17: 251–258.
- Mullany P, Williams R, Langridge GC, Turner DJ, Whalan R, et al. (2012) Behavior and target site selection of conjugative transposon Tn916 in two different strains of toxigenic *Clostridium difficile*. *Appl Environ Microbiol* 78: 2147–2153.
- Burrus V, Waldor MK (2004) Shaping bacterial genomes with integrative and conjugative elements. *Res Microbiol* 155: 376–386.
- Williams KP (2002) Integration sites for genetic elements in prokaryotic tRNA and tmRNA genes: sublocation preference of integrase subfamilies. *Nucleic Acids Res* 30: 866–875.
- Lee CA, Auchtung JM, Monson RE, Grossman AD (2007) Identification and characterization of *int* (integrase), *xis* (excisionase) and chromosomal attachment sites of the integrative and conjugative element *ICEBs1* of *Bacillus subtilis*. *Mol Microbiol* 66: 1356–1369.
- Auchtung JM, Lee CA, Monson RE, Lehman AP, Grossman AD (2005) Regulation of a *Bacillus subtilis* mobile genetic element by intercellular signaling and the global DNA damage response. *Proc Natl Acad Sci U S A* 102: 12554–12559.
- Burrus V, Pavlovic G, Decaris B, Guedon G (2002) The *ICESt1* element of *Streptococcus thermophilus* belongs to a large family of integrative and conjugative elements that exchange modules and change their specificity of integration. *Plasmid* 48: 77–97.
- Franke AE, Clewell DB (1981) Evidence for conjugal transfer of a *Streptococcus faecalis* transposon (Tn916) from a chromosomal site in the absence of plasmid DNA. *Cold Spring Harb Symp Quant Biol* 45 Pt 1: 77–80.
- Franke AE, Clewell DB (1981) Evidence for a chromosome-borne resistance transposon (Tn916) in *Streptococcus faecalis* that is capable of “conjugal” transfer in the absence of a conjugative plasmid. *J Bacteriol* 145: 494–502.
- Lee CA, Babic A, Grossman AD (2010) Autonomous plasmid-like replication of a conjugative transposon. *Mol Microbiol* 75: 268–279.
- Sitkiewicz I, Green NM, Guo N, Mereghetti L, Musser JM (2011) Lateral gene transfer of streptococcal ICE element RD2 (region of difference 2) encoding secreted proteins. *BMC Microbiol* 11: 65.
- Carraro N, Libante V, Morel C, Decaris B, Charron-Bourgoin F, et al. (2011) Differential regulation of two closely related integrative and conjugative elements from *Streptococcus thermophilus*. *BMC Microbiol* 11: 238.
- Ramsay JP, Sullivan JT, Stuart GS, Lamont IL, Ronson CW (2006) Excision and transfer of the *Mesorhizobium loti* R7A symbiosis island requires an integrase IntS, a novel recombination directionality factor RdIS, and a putative relaxase RkS. *Mol Microbiol* 62: 723–734.
- Thomas J, Lee CA, Grossman AD (2013) A conserved helicase processivity factor is needed for conjugation and replication of an integrative and conjugative element. *PLoS Genet* 9: e103198.
- Yoshida K, Yamaguchi M, Morinaga T, Kinchara M, Ikeuchi M, et al. (2008) myo-Inositol catabolism in *Bacillus subtilis*. *J Biol Chem* 283: 10415–10424.
- Crooks GE, Hon G, Chandonia JM, Brenner SE (2004) WebLogo: a sequence logo generator. *Genome Res* 14: 1188–1190.
- Auchtung JM, Lee CA, Garrison KL, Grossman AD (2007) Identification and characterization of the immunity repressor (ImmR) that controls the mobile genetic element *ICEBs1* of *Bacillus subtilis*. *Mol Microbiol* 64: 1515–1528.
- Lee CA, Grossman AD (2007) Identification of the origin of transfer (*oriT*) and DNA relaxase required for conjugation of the integrative and conjugative element *ICEBs1* of *Bacillus subtilis*. *J Bacteriol* 189: 7254–7261.
- Berkmen MB, Lee CA, Loveday EK, Grossman AD (2010) Polar positioning of a conjugation protein from the integrative and conjugative element *ICEBs1* of *Bacillus subtilis*. *J Bacteriol* 192: 38–45.
- Goranov AI, Katz L, Breier AM, Burge CB, Grossman AD (2005) A transcriptional response to replication status mediated by the conserved bacterial replication protein DnaA. *Proc Natl Acad Sci U S A* 102: 12932–12937.
- Ireton K, Grossman AD (1994) A developmental checkpoint couples the initiation of sporulation to DNA replication in *Bacillus subtilis*. *Embo J* 13: 1566–1573.
- Cheo DL, Bayles KW, Yasbin RE (1991) Cloning and characterization of DNA damage-inducible promoter regions from *Bacillus subtilis*. *J Bacteriol* 173: 1696–1703.
- Burrus V, Waldor MK (2003) Control of SXT integration and excision. *J Bacteriol* 185: 5045–5054.
- Shimada K, Weisberg RA, Gottesman ME (1972) Prophage lambda at unusual chromosomal locations. I. Location of the secondary attachment sites and the properties of the lysogens. *J Mol Biol* 63: 483–503.
- Smits WK, Grossman AD (2010) The transcriptional regulator Rok binds A+T-rich DNA and is involved in repression of a mobile genetic element in *Bacillus subtilis*. *PLoS Genet* 6: e1001207.
- Celli J, Trieu-Cuot P (1998) Circularization of Tn916 is required for expression of the transposon-encoded transfer functions: characterization of long tetracycline-inducible transcripts reading through the attachment site. *Mol Microbiol* 28: 103–117.
- Garry DB, Zahler SA (1994) Mutations in the gene for a tRNA that functions as a regulator of a transcriptional attenuator in *Bacillus subtilis*. *Genetics* 137: 627–636.
- Ho SN, Hunt HD, Horton RM, Pullen JK, Pease LR (1989) Site-directed mutagenesis by overlap extension using the polymerase chain reaction. *Gene* 77: 51–59.
- Youngman P, Poth H, Green B, York K, Olmedo G, et al. (1989) Methods for Genetic Manipulation, Cloning, and Functional Analysis of Sporulation Genes in *Bacillus subtilis*. In: Smith I, Slepceky RA, Setlow P, editors. *Regulation of Prokaryotic Development*. Washington, D.C.: ASM Press. pp. 65–87.
- Wach A (1996) PCR-synthesis of marker cassettes with long flanking homology regions for gene disruptions in *S. cerevisiae*. *Yeast* 12: 259–265.
- Miller JH (1972) *Experiments in Molecular Genetics*. Cold Spring Harbor, N.Y.: Cold Spring Harbor Laboratory. xvi, 466 p.
- Jaacks KJ, Healy J, Losick R, Grossman AD (1989) Identification and characterization of genes controlled by the sporulation-regulatory gene *spo0H* in *Bacillus subtilis*. *J Bacteriol* 171: 4121–4129.
- Glaser P, Frangeul L, Buchrieser C, Rusniok C, Amend A, et al. (2001) Comparative genomics of *Listeria* species. *Science* 294: 849–852.
- Perego M, Spiegelman GB, Hoch JA (1988) Structure of the gene for the transition state regulator, *abrB*: regulator synthesis is controlled by the *spo0A* sporulation gene in *Bacillus subtilis*. *Mol Microbiol* 2: 689–699.
- Vandeyar MA, Zahler SA (1986) Chromosomal insertions of Tn917 in *Bacillus subtilis*. *J Bacteriol* 167: 530–534.
- Smith BT, Grossman AD, Walker GC (2001) Visualization of mismatch repair in bacterial cells. *Mol Cell* 8: 1197–1206.

Author Contributions

Conceived and designed the experiments: KLM ADG. Performed the experiments: KLM. Analyzed the data: KLM ADG. Contributed reagents/materials/analysis tools: KLM. Wrote the paper: KLM ADG.